Metamaterial-inspired perfect tunnelling in semiconductor heterostructures

Metamaterial-inspired perfect tunnelling in semiconductor heterostructures

L Jelinek[1,5], J D Baena[2], J Voves[3] and R Marques[4]

[1] Department of Electromagnetic Field, Czech Technical University in Prague, Prague, Czech Republic
[2] Department of Physics, National University of Colombia, Bogota, Colombia
[3] Department of Microelectronics, Czech Technical University in Prague, Prague, Czech Republic
[4] Department of Electronics and Electromagnetism, University of Seville, Seville, Spain
E-mail: l_jelinek@us.es

Abstract. In this paper, we use a formal analogy of the electromagnetic wave equation and the Schrödinger equation in order to study the phenomenon of perfect tunnelling (tunnelling with unitary transmittance) in a one-dimensional semiconductor heterostructure. Using the Kane model of a semiconductor, we show that this phenomenon can indeed exist, resembling all the interesting features of the corresponding phenomenon in classical electromagnetism in which metamaterials (substances with negative material parameters) are involved. We believe that these results can pave the way toward interesting applications in which metamaterial ideas are transferred into the semiconductor domain.

---

[5] Author to whom any correspondence should be addressed.

IOP Institute of Physics **Φ** DEUTSCHE PHYSIKALISCHE GESELLSCHAFT

Contents

1. Introduction

The tunnelling of electrons through a potential barrier is a phenomenon that has been known to physicists for a long time [1, 2]. Initially, the tunnelling amplitudes were known to take appreciable values only on atomic scales. Later, however, use of the resonant tunnelling found in semiconductor layered structures [3] opened the way to high tunnelling amplitudes even in macroscopic devices, such as resonant tunnelling diodes.

Phenomena equivalent to quantum tunnelling are also known in other fields of physics, one example being classical electromagnetism [4]. There, for example, a section of a hollow metallic waveguide above the cutoff frequency can serve as the environment where the wave propagates, while the section of the waveguide below the cutoff frequency can serve as the potential barrier through which the photons can tunnel. In the field of electromagnetism, so-called perfect tunnelling, i.e. tunnelling with a unitary transmission coefficient, has been proposed [5], theoretically studied [6, 7] and experimentally proved [8] with the help of metamaterials [9], which are substances that at some frequency offer negative permittivity and permeability values.

The aim of this paper is to show that perfect tunnelling, like other metamaterial-inspired phenomena, such as negative refraction [10], can also exist in the quantum domain. The proposal is based on the mathematical similarity of the Schrödinger equation and the electromagnetic wave equation.

2. Maxwell–Schrödinger analogy

In order to proceed to perfect quantum tunnelling, let us first show an example of a perfect tunnelling setup in the case of electromagnetic waves. The structure is sketched in figure 1, and follows the idea presented in [6]. The layers are assumed to be laterally infinite, and the plane waves are assumed to propagate perpendicular to the layers. The structure is fed by an incident wave from vacuum region 1, which potentially also contains some reflected wave. Regions 2, 3, 4 support only evanescent waves, due to the negative values of the constitutive parameters. Any wave that tunnels the structure will appear in region 5. It has been shown [6] that it is always possible to find such d_1, d_2 for which the tunnelling (transmission) through this structure is equal to unity and can thus be called perfect, although the structure may contain potential barriers of theoretically any thickness. A realistic example of this structure has been experimentally studied [8] with the use of metamaterials. Note also that this perfect tunnelling setup is not limited to three layers. Any number of such alternating negative parameter layers can
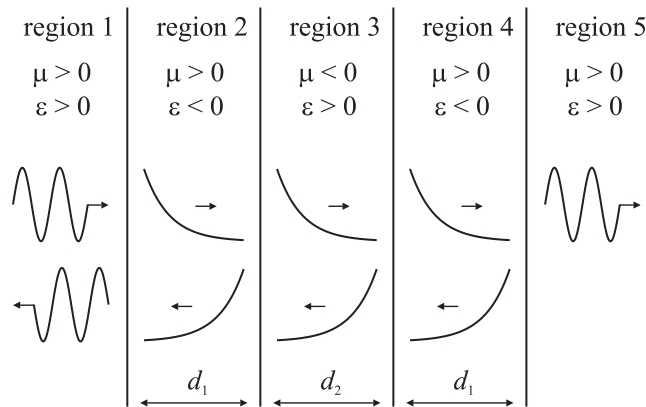
region 1	region 2	region 3	region 4	region 5
$\mu > 0$	$\mu > 0$	$\mu < 0$	$\mu > 0$	$\mu > 0$
$\varepsilon > 0$	$\varepsilon < 0$	$\varepsilon > 0$	$\varepsilon < 0$	$\varepsilon > 0$

Figure 1. Sketch of the electromagnetic perfect tunnelling setup.

be used [11, 12], leading to the same result. At this point it is important to note that the above-described perfect tunnelling is strikingly different from usual Fabry–Perot resonance, where phase propagation plays an essential role. On the contrary, in the described system, the phase propagation in regions 2, 3, 4 is null and Fabry–Perot resonance cannot occur. Furthermore, by proper settings of permittivity and permeability, the phase difference between input and output can be made zero, which is impossible in the Fabry–Perot case.

The way to transform this structure into a quantum structure uses an analogy between the electromagnetic wave equation and the Schrödinger equation [13–15]. More specifically, if the longitudinal axis in figure 1 is denoted as the z-axis, the Maxwell equations for a monochromatic plane wave with angular frequency ω propagating along this axis can be written as

$$\frac{\partial}{\partial z}\begin{bmatrix} E_x \\ H_y \end{bmatrix} = \begin{bmatrix} 0 & \mathrm{i}\omega\mu \\ \mathrm{i}\omega\varepsilon & 0 \end{bmatrix}\begin{bmatrix} E_x \\ H_y \end{bmatrix}. \tag{1}$$

Equation (1) has to be accompanied by proper boundary conditions for each boundary between different material regions, namely

$$E_x^+ = E_x^- \tag{2}$$

and

$$\frac{1}{\mu^+}\frac{\partial E_x^+}{\partial z} = \frac{1}{\mu^-}\frac{\partial E_x^-}{\partial z}. \tag{3}$$

In the uniband approximation, however, the time-independent Schrödinger equation for the wavefunction envelope ψ can be written as [16–18]

$$\frac{-\hbar^2}{2m}\frac{\partial^2 \psi}{\partial^2 z} + V\psi = E\psi, \tag{4}$$

where m is the effective mass of the particle in a given material, E is the energy of the particle, and V is the potential step on the boundary between two adjacent materials. Equation (4) can be further rewritten as

$$\frac{\partial}{\partial z}\begin{bmatrix} \psi \\ \dfrac{-\mathrm{i}\hbar}{m}\dfrac{\partial \psi}{\partial z} \end{bmatrix} = \begin{bmatrix} 0 & \mathrm{i}\dfrac{m}{\hbar} \\ 2\mathrm{i}\dfrac{(E-V)}{\hbar} & 0 \end{bmatrix}\begin{bmatrix} \psi \\ \dfrac{-\mathrm{i}\hbar}{m}\dfrac{\partial \psi}{\partial z} \end{bmatrix}, \tag{5}$$
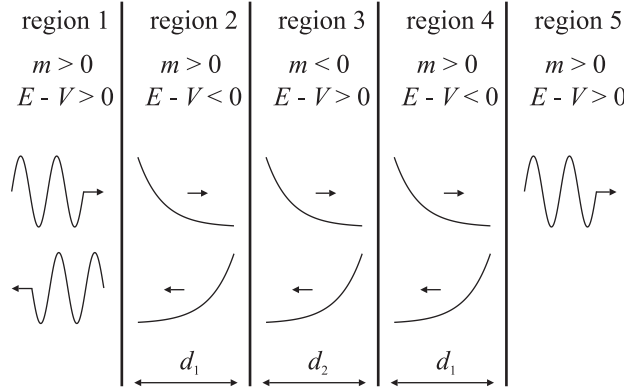
Figure 2. Sketch of the quantum perfect tunnelling setup.

and accompanied by proper boundary conditions, namely

$$\psi^+ = \psi^- \tag{6}$$

and

$$\frac{1}{m^+} \frac{\partial \psi^+}{\partial z} = \frac{1}{m^-} \frac{\partial \psi^-}{\partial z}. \tag{7}$$

Note that (7) here replaces the usual condition for continuity of the derivative. This condition arises from the electric current conservation on the material boundary [19], where the quantum analogue of the electric current density is taken as $\mathbf{j} = e\mathbf{s}$, with e as the electron charge and

$$\mathbf{s} = \frac{\hbar}{2im} \left(\psi^* \nabla \psi - \psi \nabla \psi^* \right) \tag{8}$$

as the probability density current.

Comparing (1)–(3) with (5)–(7), we can see that the Maxwell–Schrödinger analogy can be made perfect and that the solution of (1) on the structure of figure 1 will be mathematically identical with the quantum structure, where

$$E_x \to \psi; \quad \mu \to m; \quad \varepsilon \to 2(E - V); \quad \omega \to 1/\hbar. \tag{9}$$

It is also interesting to note that (8) gives another part of the Maxwell–Schrödinger analogy, namely the analogy of the Poynting vector and the probability density current:

$$\mathrm{Re}\left[E_x H_y^*\right] \to s_z. \tag{10}$$

3. Theoretical analysis

We are thus about to study the structure shown in figure 2. Unfortunately, being rigorous, (4) is not valid in any realistic semiconductor heterostructure. In fact, the heterostructure of two materials A and B would be better described by the 8×8 Kane [20, 21] model:

$$\left[E_{l0} - \frac{\hbar^2}{2m_0} \frac{\partial^2}{\partial z^2}\right] f_l(z) + \sum_{m=1}^{8} \frac{1}{m_0} \langle u_{l0}| \frac{\hbar}{i} \frac{\partial}{\partial z} |u_{m0}\rangle \frac{\hbar}{i} \frac{\partial f_m(z)}{\partial z} = E f_l(z) \tag{11}$$

with $l = 1, \ldots, 8$, E_{l0} as the double degenerate (spin) band edge energies (for $k = 0$) of the conduction, light hole valence, heavy hole valence and split off valence bands (E_{l0} is different

for materials A and B), $f_l(z)$ as the corresponding envelope functions, m_0 as the electron mass and u_{l0} as the bulk material eigenfunctions for the mentioned bands at $k = 0$ that are assumed to be the same in the entire heterostructure. In the following, we will denote the eight band edge states by their symmetry properties: Γ_6 as an s-like state with eigenvalues of angular momentum $J = 1/2$, $J_z = \pm 1/2$, Γ_8 as a p-like state with $J = 3/2$, $J_z = \pm 1/2, \pm 3/2$ and Γ_7 as a p-like state with $J = 1/2$, $J_z = \pm 1/2$.

The matrix system (11) represents the multiband nature of semiconductors, a phenomenon that is not present in our electromagnetic problem. However, it has been shown [21, 22] that the different spin states are not coupled in this model, and so the 8×8 system can be directly reduced into two identical 4×4 systems. In addition, the heavy hole states are uncoupled to the three light states (electron, light hole, split off hole), and thus the 4×4 system can be directly separated into one heavy hole scalar equation and a 3×3 matrix system for the light states. Finally, under a very reasonable approximation [22] of dropping the free space kinetic term in the light hole and split off hole state equations (a very good approximation for the energy and wave vector range of our interest), the 3×3 light states matrix system can be solved for conduction states, leading to the scalar equation

$$\left[-\frac{\hbar^2}{2m} \frac{\partial^2}{\partial z^2} + E_{\Gamma_6} \right] f_c(z) = E f_c(z) \tag{12}$$

where

$$\frac{1}{m} = \frac{2P^2}{3} \left[\frac{2}{E - E_{\Gamma_8}} + \frac{1}{E - E_{\Gamma_7}} \right] \tag{13}$$

is the energy- and position-dependent effective mass. The quantities E_{Γ_6}, E_{Γ_8} and E_{Γ_7} are the band edge energies of the Γ_6, Γ_8 and Γ_7 bands, which are position dependent in a step-like manner along the heterostructure. The quantity $P = \frac{-i}{m_0}\langle S| \frac{\hbar}{i} \frac{\partial}{\partial x} |X\rangle = \frac{-i}{m_0}\langle S| \frac{\hbar}{i} \frac{\partial}{\partial y} |Y\rangle = \frac{-i}{m_0}\langle S| \frac{\hbar}{i} \frac{\partial}{\partial z} |Z\rangle$ is the element of the Kane matrix where $|S\rangle$, $|X\rangle$, $|Y\rangle$ and $|Z\rangle$ represent the s-like and the three p-like eigenfunctions for $k = 0$.

The envelope equation (12) is accompanied by appropriate boundary conditions, which read

$$f_c(z^+) = f_c(z^-) \tag{14}$$

and

$$\frac{1}{m^+} \frac{\partial f_c(z^+)}{\partial z} = \frac{1}{m^-} \frac{\partial f_c(z^-)}{\partial z}. \tag{15}$$

Thus, the equation for $f_c(z)$ and its boundary conditions are analogous to (4), (6) and (7), with the only difference being that the effective mass is now a function of the energy and some adjustable parameters.

Before moving to practical implementation, it is worth mentioning that the simple Kane model presented above is mostly qualitative. Its qualitative validity has been confirmed in the past by a more sophisticated tight binding method [23, 24]; however, quantitative differences from reality are expected.

4. Practical implementation

Comparing the scheme of figure 2 with the above-mentioned mathematical formalism, we can arrive at a possible implementation of the perfect tunnelling setup using the $Hg_{1-x}Cd_xTe$ ternary
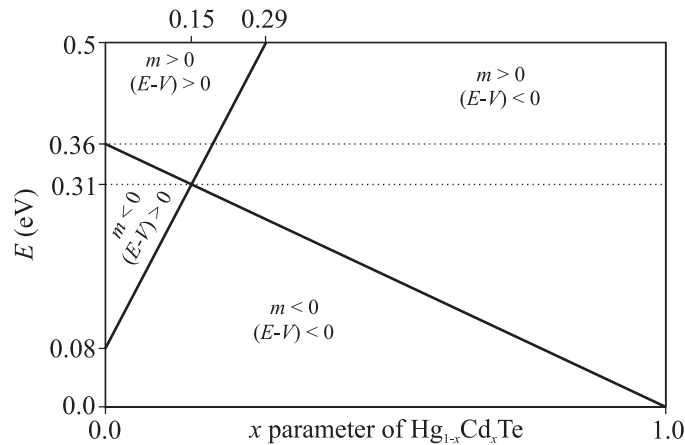
Figure 3. $E-x$ plane of $Hg_{1-x}Cd_xTe$ ternary alloy. The solid lines correspond to E_{Γ_6} and E_{Γ_8} as functions of mixing parameter x and divide the plane into four fields with different signs of mass and energy difference. The dotted lines define the band of energies of possible perfect tunnelling.
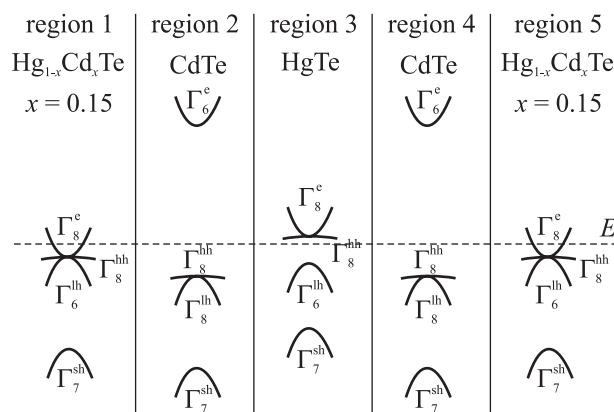

Figure 4. Band diagram sketch of the realistic quantum tunnelling structure. Note that in regions 2, 3, 4 the energy line lies inside the bandgap.

alloy. The heterostructures of this alloy have been extensively studied [25–27] for the possibility of the existence of interface states that are indeed closely related to the perfect tunnelling. The parameters needed for calculating the envelope function via (12) and (13) can be obtained from reliable measurements or from first principles calculations [28–30], which suggest $2m_0P^2 \approx 18.5\,\text{eV}$, $E_{\Gamma_6} \approx (1.47x + 0.08)\,\text{eV}$, $E_{\Gamma_8} \approx (-0.36x + 0.36)\,\text{eV}$ and $E_{\Gamma_7} \approx (-0.36x - 0.59)\,\text{eV}$, where x represents the $Hg_{1-x}Cd_xTe$ mole fraction. These values are also in agreement with a recent review [31] of HgCdTe alloys.

The possibilities of the $Hg_{1-x}Cd_xTe$ alloy are graphically represented in figure 3. The proposed perfect tunnelling requires three different combinations of m and $(E - V)$ at a given energy value, a condition that is satisfied for any energy between the two dotted lines in figure 3. An obvious possibility is thus the setup depicted in figure 4, which is also the setup with the highest energy band of operation, thus allowing a looser choice of structural dimensions.
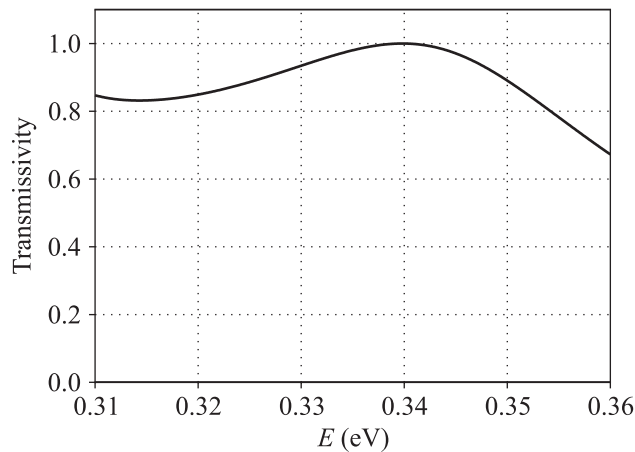
Figure 5. Amplitude of the transmission coefficient through the structure of figure 4 for $d_1 = 1.26$ nm, $d_2 = 10$ nm.
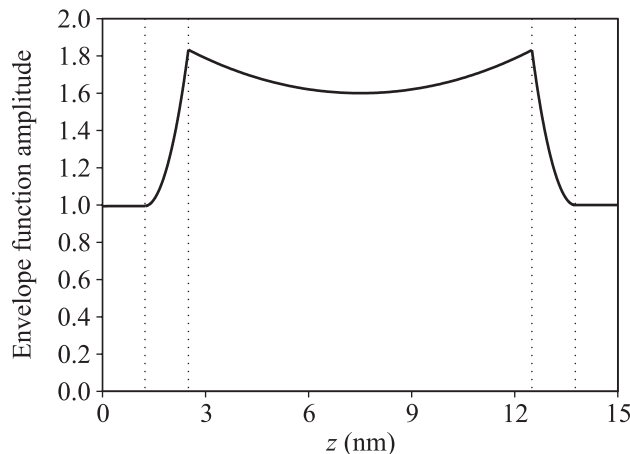

Figure 6. Amplitude of the envelope function (12) in the structure of figure 4 for the energy of maximum transmittance.

The transmission coefficient in the perfect tunnelling energy band and the amplitude of the envelope function at the transmission maximum were calculated for $d_1 = 1.26$ nm, $d_2 = 10$ nm, and are depicted in figures 5 and 6. The transmission coefficient was obtained by the transfer matrix method and the envelope function amplitude was obtained by backward unfolding of the matrix cascade. The dimensions were chosen so that the perfect tunnelling occurs at $E = 0.34$ eV, which corresponds to the effective mass and potential difference in each layer [m, E_{Γ_6}] given by [$0.0027\,m_0$, 0.30 eV], [$0.024\,m_0$, 1.55 eV], [$-0.0016\,m_0$, 0.08 eV] for regions 1 (5), 2 (4), 3, respectively. Any reasonably small change in dimensions will lead to a shift in the tunnelling energy; however, at that energy the phenomenon will be the same. This means that in the real experiment the structural dimensions need only be moderately precise, but the source has to be fine tuned in energy.

Both figures 5 and 6 clearly present the perfect tunnelling that we are looking for, including the interface states maxima [25–27] at the boundaries where the effective mass changes its

sign. By analogy with the electromagnetic problem, it can also be shown that at the energy of unitary transmittance the probability density current (8) will be constant along the whole heterostructure. At this point it is important to stress that unitary transmission is achieved at energies for which regions 2, 3, 4 support only evanescent waves. This phenomenon is thus very different from the usual resonant tunnelling, for which region 3 is propagative with either $m > 0$, $(E - V) > 0$ (resonant tunnelling diode) or $m < 0$, $(E - V) < 0$ (interband resonant tunnelling diode).

5. Conclusions

In summary, we have exploited the formal analogy of the electromagnetic wave equation and the Schrödinger equation to transfer the idea of electromagnetic perfect tunnelling into the semiconductor domain. Using the well-accepted Kane model of a semiconductor, we have particularly shown that perfect tunnelling can be found in one-dimensional semiconductor heterostructures composed of HgCdTe ternary alloys exhibiting all the features of the electromagnetic phenomenon. We think that the results reported here can stimulate greater interest in extending the physical concept of metamaterials into the semiconductor domain, leading to interesting new applications.

Acknowledgments

References

[1] Gamow G 1928 Zur quantentheorie des atomkernes *Z. Phys.* **51** 204
[2] Gurney R W and Condon E U 1929 Quantum mechanics and radioactive disintegration *Phys. Rev.* **33** 127
[3] Esaki L and Tsu R 1970 Superlattice and negative differential conductivity in semiconductors *IBM J. Res. Dev.* **14** 61
[4] Jackson J D 1998 *Classical Electrodynamics* 3rd edn (New York: Wiley)
[5] Pendry J B 2000 Negative refraction makes a perfect lens *Phys. Rev. Lett.* **85** 3966
[6] Alu A and Engheta N 2003 Pairing an epsilon-negative slab with a mu-negative slab: resonance, tunneling and transparency *IEEE Trans. Antennas Propag.* **51** 2558
[7] Smith D R and Schurig D 2003 Electromagnetic wave propagation in media with indefinite permittivity and permeability tensors *Phys. Rev. Lett.* **90** 077405
[8] Baena J D, Jelinek L, Marques R and Medina F 2005 Near-perfect tunneling and amplification of evanescent electromagnetic waves in a waveguide filled by a metamaterial: theory and experiments *Phys. Rev.* B **72** 075116
[9] Marqués R, Martín F and Sorolla M 2007 *Metamaterials with Negative Parameters: Theory and Microwave Applications* (New York: Wiley)
[10] Cheianov V V, Falko V and Altshuler B L 2007 The focusing of electron flow and a veselago lens in graphene p–n junctions *Science* **315** 1252

[11] Shamonina E, Kalinin V A, Ringhofer K H and Solymar L 2001 Electromagnetic interaction of parallel arrays of dipole scatterers *Electron. Lett.* **37** 1243

[12] Baena J D, Jelinek L and Marques R 2005 Reducing losses and dispersion effects in multilayer metamaterial tunnelling devices *New J. Phys.* **7** 166

[13] Gaylord T K, Henderson G N and Glytsis E N 1993 Application of electromagnetics formalism to quantum-mechanical electron-wave propagation in semiconductors *J. Opt. Soc. Am.* B **10** 333

[14] Dragoman D and Dragoman M 1999 Optical analogue structures to mesoscopic devices. *Prog. Quantum Electron.* **23** 131

[15] Dragoman D and Dragoman M 2007 Metamaterials for ballistic electrons *J. Appl. Phys.* **101** 104316

[16] Wannier G H 1937 Structure of electronic excitation levels in insulating crystals *Phys. Rev.* **52** 191

[17] Slater J C 1949 Electrons in perturbed periodic lattices. *Phys. Rev.* **76** 1592

[18] Ben Daniel D J and Duke C B 1966 Space-charge effects on electron tunneling *Phys. Rev.* **152** 683

[19] Harrison W A 1961 Tunneling from an independent-particle point of view *Phys. Rev.* **123** 85–9

[20] Kane E O 1957 Band structure of indium antimonide *J. Phys. Chem. Sol.* **1** 249

[21] Bastard G 1988 *Wave Mechanics Applied to Semiconductor Heterostructures* (New York: Interscience Wiley-Interscience)

[22] Bastard G 1982 Theoretical investigations of superlattice band structure in the envelope-function approximation *Phys. Rev.* B **25** 7584

[23] Schulman J N and Chang Y-C 1986 HgTe–CdTe superlattice subband dispersion *Phys. Rev.* B **33** 2594

[24] Fornari M, Chen H H, Fu L, Graft R D, Lohrmann D J, Moroni S, Pastori Parravicini G, Resca L and Stroscio M A 1997 Electronic structure and wave functions of interface states in HgTe–CdTe quantum wells and superlattices *Phys. Rev.* B **55** 16339

[25] Guldner Y, Bastard G, Vieren J P, Voos M, Faurie J P and Million A 1983 Magneto-optical investigations of a novel superlattice: HgTe-CdTe *Phys. Rev. Lett.* **51** 907

[26] Chang Y-C, Schulman J N, Bastard G, Guldner Y and Voos M 1985 Effects of quasi-interface states in HgTe–CdTe superlattices *Phys. Rev.* B **31** 2557

[27] Lin-Liu Y R and Sham L J 1985 Interface states and subbands in HgTe–CdTe heterostructures *Phys. Rev.* B **32** 5561

[28] Kowalczyk S P, Cheung J T, Kraut E A and Grant R W 1986 CdTe-HgTe (111) heterojunction valence-band discontinuity: a common-anion-rule contradiction *Phys. Rev. Lett.* **56** 1605

[29] Johnson N F, Hui P M and Ehrenreich H 1988 Valence-band-offset controversy in HgTe/CdTe superlattices: a possible resolution *Phys. Rev. Lett.* **61** 1993

[30] Mecabih S, Amrane N, Belgoumene B and Aourag H 2000 Opto-electronic properties of the ternary alloy $Hg_{1-x}Cd_xTe$ *Physica* A **276** 495

[31] Rogalski A 2005 HgCdTe infrared detector material: history, status and outlook *Rep. Prog. Phys.* **68** 2267